doi:10.1093/scan/nsu013 SCAN (2014) 9, 1993–2000

# Escape from harm: linking affective vision and motor responses during active avoidance

**Vladimir Miskovic**[1,2] **and Andreas Keil**[1,3]

[1]Center for the Study of Emotion and Attention, University of Florida, Gainesville, FL 32608, [2]Department of Psychology, State University of New York at Binghamton, Binghamton, NY 13902-6000, USA, and [3]Department of Psychology, University of Florida, Gainesville, FL 32611

**When organisms confront unpleasant objects in their natural environments, they engage in behaviors that allow them to avoid aversive outcomes. Here, we linked visual processing of threat to its behavioral consequences by including a motor response that terminated exposure to an aversive event. Dense-array steady-state visual evoked potentials were recorded in response to conditioned threat and safety signals viewed in active or passive behavioral contexts. The amplitude of neuronal responses in visual cortex increased additively, as a function of emotional value and action relevance. The gain in local cortical population activity for threat relative to safety cues persisted when aversive reinforcement was behaviorally terminated, suggesting a lingering emotionally based response amplification within the visual system. Distinct patterns of long-range neural synchrony emerged between the visual cortex and extravisual regions. Increased coupling between visual and higher-order structures was observed specifically during active perception of threat, consistent with a reorganization of neuronal populations involved in linking sensory processing to action preparation.**

**Keywords:** aversive conditioning; avoidance; threat processing; EEG; functional connectivity; visual cortex

## INTRODUCTION

The traditional view that activity in the sensory cortex instantiates invariant representations of external stimuli is being replaced by an emerging consensus that sensory networks are best characterized as adaptive processors whose responses are continuously shaped by an individual's learning history and current behavioral state (Engel *et al.*, 2001, 2013; Freeman, 2001; Gilbert and Sigman, 2007). Sensory features that have been associated with affective value in the past lead to more vigorous neuronal responses compared with other stimuli that are neutral in their emotional tone (Lang and Bradley, 2010). Sensory tuning for affectively salient stimuli represents a highly conserved biological phenomenon that is observed not only in diverse mammalian species (Weinberger, 2004) but also in invertebrates (van Swinderen and Greenspan, 2003) and very likely emerges at the earliest stages of stimulus contact (Barrett and Bar, 2009).

The visual processing of danger cues, in particular, is the first step in a cascade of events that transpire between the registration of emotional significance and behavioral responses directed back into the environment. When organisms confront aversive stimuli, they engage in defensive behaviors that minimize contact with the noxious elements. Most laboratory models of aversive conditioning in humans do not attempt to model the behavioral inclinations of natural agents—namely, to escape sources of harm and seek safety (Beckers *et al.*, 2013). The capacity to avoid harmful outcomes alters the behavioral and affective context within which threat cues are perceived by making the stimulus-outcome contingency dependent on the individual's actions, rather than reflecting a fixed statistical relation. Recent empirical evidence has demonstrated the sensitivity of visual cortical response profiles to different behavioral contexts in rodents (Niell and Stryker, 2010) and primates (Lee *et al.*, 2002; Mirabella *et al.*, 2007). For instance, different responses of visual cortical neurons are observed in macaque monkeys when contrasting passive viewing with viewing under conditions of self-initiated movement (Gallant *et al.*, 1998). An outstanding question concerns the degree to which population-level visual cortical activity in humans is modified by defensive behaviors aimed at altering the emotional significance of a visual stimulus.

When laboratory animals are permitted to emit behavioral responses that allow them to avoid negative outcomes (e.g. footshock) which would normally follow conditioned danger cues, they learn such responses relatively rapidly with the underlying neural activity being diverted from brainstem regions that mediate innate defensive reactions (e.g. freezing and defecation) to a more distributed brain network that permits active coping behaviors (LeDoux and Gorman, 2001). In humans, termination of unpleasant events induces feelings of safety (Lohr *et al.*, 2007) and has been found to activate brain regions, such as the medial orbitofrontal cortex, that normally track the rewarding qualities of stimuli (Kim *et al.*, 2006). Human participants rate conditioned threat cues as less aversive and exhibit reduced sweat gland activity, when they are provided with an opportunity to avoid negative outcomes (Szpiler and Epstein, 1976; Lovibond *et al.*, 2008; Delgado *et al.*, 2009). However, hemodynamic imaging has revealed residual activity in amygdala-based defensive circuits in response to threat-related cues, even when individuals are able to avoid aversive outcomes (Delgado *et al.*, 2009; Schlund and Cataldo, 2010; Schlund *et al.*, 2010, 2013). Given these varied findings, it remains unclear how active avoidance influences neural processes in humans that are central to sensory engagement and behavioral confrontation with aversive stimuli.

The primary goal of this study was to examine how the visual brain would respond to conditioned threat cues when participants could actively emit responses to avoid harmful outcomes in contrast to situations where the outcome was inescapable. We examined the macroscopic responses of visual cortical regions by recording a measure of population-level neuronal activity, the steady-state visual evoked potential (ssVEP). The ssVEP consists of brain oscillatory responses entrained by a rhythmically modulated visual stream (Regan, 1989; Vialatte *et al.*, 2010). Owing to their narrow band manifestation, ssVEPs possess excellent signal-to-noise ratios compared with traditional ERP components (Nunez and Srinivasan, 2006). Fluctuations in ssVEP amplitude provide sensitive indices of activity in visual neuron populations (Müller *et al.*, 1998; Tononi *et al.*, 1998;

Received 14 July 2013; Revised 12 November 2013; Accepted 10 January 2014
Advance Access publication 3 February 2014

This research was supported by grants from NIMH (R01 MH084932–02 and R01 MH097320) and from the US AMRAA (W81XWH-11-2-0008) awarded to A.K. and by a fellowship from the Canadian Institutes of Health Research (CIHR) awarded to V.M.

Correspondence should be addressed to Vladimir Miskovic, Department of Psychology, State University of New York at Binghamton, Binghamton, NY 13902-6000, USA. E-mail: miskovic@binghamton.edu

Andersen and Müller, 2010). An added advantage of the ssVEP method is the ability to use frequency-based tagging of neuronal responses to discriminate reactivity to spatially and temporally overlapped stimuli (e.g. Müller *et al.*, 2008; Wieser and Keil, 2011). Here, we exploited the unique properties of ssVEP methodology to distinguish neural reactivity to discrete stimuli conveying information about emotional significance and behavioral relevance.

To complement analyses of local cortical population activity within visual regions, we also examined the amount of long-range synchronization between estimated cortical sources oscillating specifically at the stimulation frequencies. Analyses of functional connectivity provide a window into how regions outside of the visual cortex coalesce into large-scale networks that integrate the perception of stimuli with attentive behavior and response orchestration.

Our experimental design allowed us to test two main competing hypotheses. According to the first hypothesis and consistent with previous studies of autonomic reflex function (e.g. Lovibond *et al.*, 2008), the ability to actively avoid negative outcomes should suppress response enhancement for threat-relevant cues as their emotional significance is decreased. In contrast, a second hypothesis, consistent with recent functional MRI (fMRI) findings (e.g. Schlund *et al.*, 2013), predicts persistent vigilance for threat-related cues, even when one can alter the environment so as to avoid the negative outcome. Overall, as suggested by the previous literature, we expected that viewing stimuli in the context of active behavioral responses would evoke greater engagement of visual cortical regions and increased long-range synchronization between sensory and motor regions compared with passive viewing alone.

## METHODS

### Participants

A total of 18 participants were recruited from a pool of undergraduate students and participated for course credit. Of these 18 participants, three were excluded for the following reasons: (i) non-compliance with experiment instructions ($n = 1$) and (ii) failure to obtain a reliable ssVEP response for peripheral cue stimuli ($n = 2$). Following these exclusions, data from 15 participants (eight females, seven males, M age = 18.47 years, s.d. = 0.74 years) were retained for subsequent analyses.

### Stimuli

The visual stimuli were generated using the Psychophysics Toolbox (Brainard, 1997) for MATLAB. They consisted of black-and-white sinusoidal gratings (Gaussian-windowed with maximal contrast at center) subtending horizontal and vertical visual angles of 7°. The CS+ and CS− gratings were low in spatial frequency (1.4 cycles per degree) and differed from each other only in their degrees of offset from the vertical meridian: 45° clockwise tilt (CS+) or 45° anticlockwise tilt (CS−).

The UCS was a 1 s continuous white noise burst, generated in MATLAB and presented at 92 dB sound pressure level through free-field speakers surrounding the participant. During reinforced trials, the CS+ and UCS were temporally overlapped during the last second of viewing and the two stimuli co-terminated (i.e. delay conditioning preparation).

### Procedure

After providing written informed consent and initial screening to rule out photic epilepsy/seizures, participants were seated in a dimly lit testing room where the electroencephalogram (EEG) sensor net was applied and participants were given instructions to fixate, avoid eye movements and blinks, and to expect occasional loud noises. Stimuli were displayed on a 21 in. display LED monitor with a 120 Hz refresh rate, positioned at a distance of 1 m. To facilitate learning the CS–UCS contingencies and the instrumental response, we employed an instructed differential conditioning design that included one grating stimulus (the CS+) that was aversively reinforced and another grating with a different orientation (the CS−) that was never reinforced. Verbal instructions constitute a potent route for the acquisition of aversive learning in humans (Rachman, 1977).

Participants first underwent an initial habituation phase, during which they were passively exposed to 10 presentations of each grating. Reinforcement rate was set at 0% for the initial habituation block. Participants then entered the conditioning phase of the experiment during which the 10 CS+ trials were accompanied by UCS delivery, with a 100% reinforcement rate; the 10 CS− trials were never reinforced. The avoidance phase followed the initial conditioning block and forms the basis of the present report (see Figure 1 for the experimental schematic). The CS+ and CS− gratings were presented centrally and flickered at 15 Hz (square wave luminance modulation). The avoidable *vs* unavoidable context was signaled by additional geometric shapes that flanked the centrally displayed conditioned stimuli, in a fully balanced design: CS+ active trials (appropriate motor response cancels UCS delivery), CS+ passive trials (no motor response is required and UCS delivery is inevitable), CS− active trials (appropriate motor response is required, but UCS is never delivered) and CS− passive trials (no motor response is required and UCS is never delivered). The cues that signaled trial type were perceptually unique and flickered at a different fundamental frequency (12 Hz) from the conditioned stimuli. A salient color change of the peripheral cues, from gray to green, that occurred halfway within each trial (3 s from stimulus onset with a 2 s duration) served as the proximal impetus for motor responses. A simple button press during a circumscribed temporal window (the 'green' period) successfully cancelled delivery of the white noise ('active CS+' condition); in contrast, white noise delivery was inevitable on another subset of trials ('passive CS+' condition). Participants were instructed to respond to the color change during the 'active CS−' trials as well but were informed that regardless of their response, the loud noise would never be presented. Given the complexity of the experimental design, and previous findings showing comparable ssVEP results for instructed and uninstructed aversive learning (Moratti and Keil, 2005; Moratti *et al.*, 2006), participants were explicitly informed (i) about which grating predicts the aversive sound and (ii) the appropriate response (action or no action) that was required on the active *vs* passive trials. Motor responses were made by the participants' dominant hand.

Peripheral cues were located ~1.7° of visual angle from the central grating stimuli and subtended visual angles of 1.5°. Following completion of the avoidance phase, participants were asked to provide a subjective estimate of the amount of distress that they experienced when encountering each of the possible CS Type and peripheral cue combinations. Participants indicated their answers by dragging a computer mouse across the horizontal plane of display and clicking anywhere on a range from 'completely relaxed' to 'highly distressed'. A brief extinction phase followed the ratings, which involved eight unreinforced presentations of the CS+ grating.

Stimulus presentation (CS+ *vs* CS− and active *vs* passive) was pseudo-randomized in each phase such that no more than two identical trial types were ever presented in succession. Trials were 6 s in length and the inter-trial interval varied randomly between 4 and 5 s. All procedures were approved by the local institutional review board of the University of Florida and were in line with the Declaration of Helsinki.

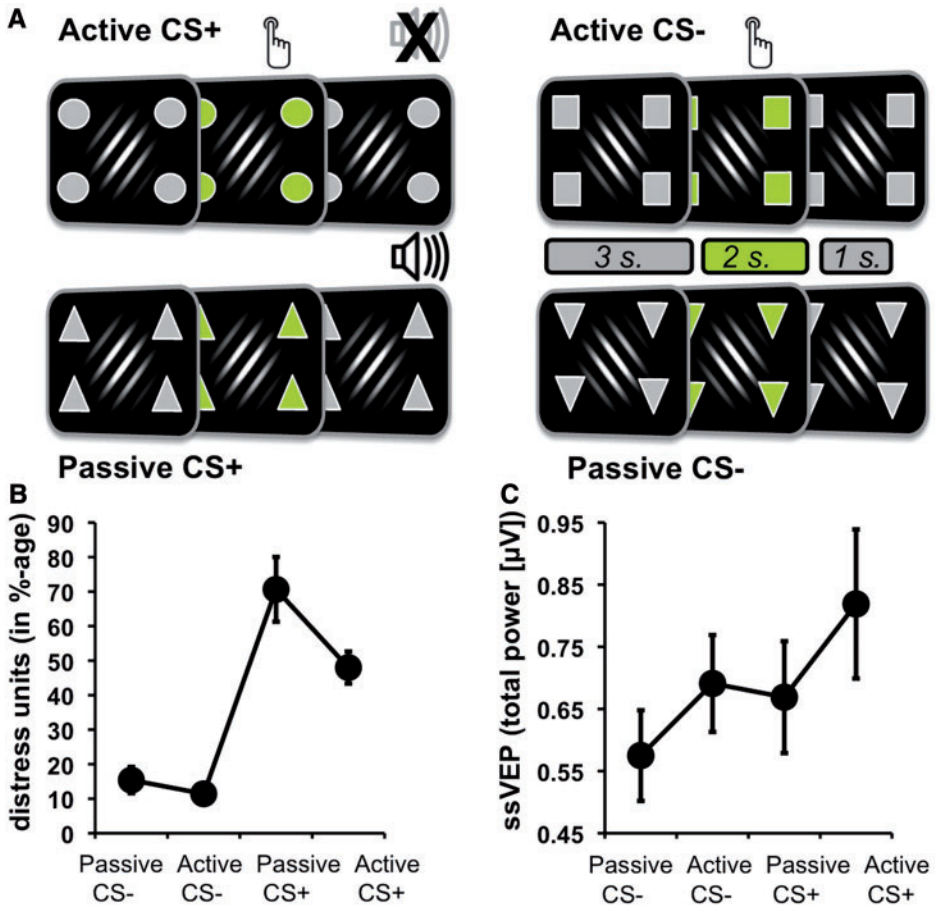


**Fig. 1** (**A**) Schematic depiction of the avoidance phase. The CS+ trials were paired with delivery of an aversive loud noise. Importantly, participants could cancel delivery of the loud sound on the active CS+ trials by a simple button press. The CS− trials were never aversively reinforced, but the active trials still required a motor response. The geometric shapes presented in the periphery indicated the type of trial. A salient color change of the geometric shape approximately halfway through a trial served as the proximal cue for action on the active trials; passive trials also involved a color change but did not require a motor response. (**B**) Mean distress ratings after conversion to percentage values. Statistical analyses were performed on raw values reflecting horizontal pixel dimensions of the display panel used to complete the ratings. Bars depict ± 1 s.e.m. (**C**) Total ssVEP amplitude combining both of the tagged stimuli (CS and action cues) together. Bars depict ± 1 s.e.m.

### EEG data recording

EEG was continuously recorded from 129 sensors using an Electrical Geodesics™ HydroCel Geodesic Sensor Net, digitized at a rate of 250 Hz, using the vertex sensor (Cz) as the recording reference, with the online band-pass filter set at 50 Hz (low-pass). Sensor impedances were kept below 50 kΩ.

### EEG data reduction and analyses

Offline EEG processing was implemented using the ElectroMagnetoEncephalography (EMEGS) toolbox for MATLAB (Peyk *et al.*, 2011). Relative to stimulus onset, epochs were extracted from the raw EEG that included 400 ms pre- and 6000 ms post-onset for all conditions. Data were filtered using a 30 Hz low-pass (45 dB/octave, 16th order Butterworth) and a 1 Hz high-pass (18 dB/octave, 4th order Butterworth). As outlined elsewhere (Junghöfer *et al.*, 2000), statistical parameters were used to find and remove artifact-contaminated channels and trials. The original recording reference (Cz) was first used to detect recording artifacts, and then the data were average referenced to detect global artifacts. Subsequently, bad sensors within individual trials were identified and interpolated based on rejection criteria for the mean absolute (rectified) amplitude, the variability over time points and the maximum first order derivate (gradient).

The artifact-free data were submitted to a Discrete Fourier Transform in MATLAB with segments extracted from 1000 to 6000 ms post-stimulus onset. The first second of the visual evoked response was not included in the main analyses in order to exclude initial non-stationary ERP components of the brain response from the power spectrum. The amplitude of ssVEP responses was quantified as the absolute value of the Fourier coefficients at the respective driving frequencies (12 and 15 Hz), normalized by signal duration and multiplied by 2 to correct for Fourier symmetry. The resulting posterior ssVEP amplitudes (in μV) were averaged across a cluster of parieto-occipital sensors (corresponding to HydroCel sensors #60, 67, 72, 77, 85, 66, 71, 76, 84, 70, 75 and 83). Our main focus was on the avoidance phase of the experiment; the habituation and conditioning phases were included only to establish initial CS-outcome associations before proceeding to the main, avoidance phase of the experiment.

### EEG source analysis

Cortical ssVEP generators were estimated using the L2 minimum norm estimate for each individual participant, following an established approach (Hauk *et al.*, 2002) and implemented in MATLAB. A total of 655 source locations (i.e. the model sources) were distributed equidistantly over a source space consisting of four concentric spherical shells. Currents at each source location were modeled for three orthogonal spatial orientations (one radial, two tangential relative to the scalp surface). As EEG is most sensitive to radial currents, the present source space analyses focused on the radial component. The four

shells had radii of 0.8, 0.6, 0.4 and 0.2 relative to the sensor radius of 1. The Tikhonov–Philips approach was used for regularization purposes in order to suppress uncorrelated noise (Hauk, 2004). A regularization factor (lambda) of 0.001 was used throughout (see Hauk, 2004 for a discussion on regularization). From the source space, the shell at 0.6 of the electrode radius was selected as a compromise between depth sensitivity and spatial resolution (Hauk *et al.*, 2002). After calculation of the inverse solutions, the 655 model sources were reduced by selecting the 129 sources located closest to the sensor positions for mapping and statistical analyses.

### ssVEP phase analyses

To examine stimulus-driven changes in long-range oscillatory synchronization, we calculated the averaged difference in phase angles between a seed visual region (corresponding to the visual midline and its four nearest neighbors) and all other sources. These analyses were performed at the source level in order to minimize spurious estimates of functional connectivity due to high field spread in scalp EEG data (Schoffelen and Gross, 2009). Extraction of inter-site phase synchrony was performed on the time-domain averaged (evoked) EEG data separately for the 12 and 15 Hz ssVEP driving frequencies using in-house written MATLAB code, resulting in a measure of inter-site phase stability during the course of ssVEP stimulation. The windowed Fourier decomposition technique used here is described extensively elsewhere (Keil *et al.*, 2008). Briefly, rather than estimating spectral power, we extracted estimates of inter-site phase synchrony among subsequent ssVEP cycles obtained from the averaged ssVEPs. An epoch window containing four cycles of each respective stimulus oscillation was shifted over the averaged ssVEP in steps equal to the single cycle of the driving frequency. Complex, unit normalized phase differences between source locations were then calculated for each epoch and averaged across using the inter-site phase synchrony algorithm proposed elsewhere (Lachaux *et al.*, 1999). The resulting values provide an index of evoked phase synchrony between the selected seed and all other regions, and are expressed on a scale from 0 (absence of phase synchronization) to 1 (maximal phase synchronization). To ensure that four cycles of the 12 and 15 Hz oscillations could be accommodated by integer multiples of the sampling period, the artifact-free EEG data were first digitally up-sampled to 600 Hz.

### Statistical approach

To test the main hypotheses relevant to how active termination of a noxious event influences visual processing of a conditioned threat cue, we conducted repeated measure analyses of variance (ANOVAs) using the within-subject factors of CS Type (CS+/CS−) and Trial Type (Active/Passive) on ssVEP power. We first focused on global modulations of ssVEP amplitude by combining the two different frequency tagged neuronal responses in order to assess overall changes in visual cortical engagement for the compound stimulus arrays. In a subsequent analysis step, we exploited the specific frequency following neuronal responses at 12 and 15 Hz to isolate the processing of conditioned gratings and action cues.

The employment of the frequency tagging technique allowed us to examine additional questions of interest, related to competition for neuronal resources within the visual cortex, between the conditioned stimuli and the peripheral response-type (active *vs* passive) cues. For these exploratory analyses, separate repeated measure ANOVAs were conducted for the CS+ and CS− trials (collapsing across active and passive conditions) and the active/passive trials (collapsing across CS+ and CS− categories). These analyses were focused on the latter half of the trial period, following the color change of peripheral cues that initiated the opening of a response window on the active trials. The within-subject factors included CS Type (or Trial Type) and Tagged Stimulus (12/15 Hz tags).

To identify task-dependent differences in the spatial topography of long-range phase synchronization patterns (referenced to visual cortex), we used permutation-corrected *t*-maps. The permutation approach allowed a powerful method of controlling for multiple statistical comparisons (Blair and Karniski, 1993). The following analyses were focused on the latter portion of the trials, when the peripheral action cues changed in color and became proximal response cues. By measuring the degree of cross-regional phase synchronization of the evoked visual response, we aimed to capture the formation of functional brain networks during the active phase of the conditioned avoidance experiment. Paired sample *t*-test contrasts were calculated on Fisher's-*Z* transformed phase synchrony measures at each source location for the comparisons of interest. Significance thresholds were then determined for each contrast by calculating 8000 topographies on random permutations of the existing data, shuffled across conditions. The maximum statistic for each topography was entered into a reference distribution, where the 5% tails served as the statistical significance criterion. For each tagged stimulus (i.e. the 12 Hz action cues and the 15 Hz conditioned gratings), we conducted a set of contrasts that isolated effects due to CS Type and Trial Type (i.e. active CS+ *vs* active CS−, passive CS+ *vs* passive CS−, active CS+ *vs* passive CS+ and active CS− *vs* passive CS−).

## RESULTS

### Behavioral findings

As a manipulation check to ensure that the instructed conditioning procedure was effective, we collected participant rated units of distress in response to the four different configurations of conditioned gratings and peripheral cues. Main effects of CS Type [$F(1,14) = 62.68$, $P < 0.001$, $\eta_p^2 = 0.82$] and Trial Type [$F(1,14) = 6.43$, $P = 0.024$, $\eta_p^2 = 0.32$] were subsumed under a CS Type × Trial Type interaction [$F(1,14) = 4.26$, $P = 0.058$, $\eta_p^2 = 0.23$]. As depicted in Figure 1B, CS+ trials were experienced as more distressing when white noise delivery was unavoidable compared with the CS+ trials where a motor response cancelled aversive noise delivery [$F(1,14) = 6.21$, $P = 0.026$, $\eta_p^2 = 0.31$]. No such differences ($P > 0.29$) between the active and passive conditions were evident for the safe, CS− trials.

Inspection of the means suggested that participants were somewhat more likely to emit motor responses on the active CS+ (M hit rate = 96%, s.e.m. = 2%) compared with the active CS− trials (M hit rate = 83%, s.e.m. = 7%). However, there was no statistically reliable difference in rates of responding between the two conditions [$F(1,14) = 3.18$, $P = 0.096$, $\eta_p^2 = 0.19$].

### Local population activity in visual cortex

Analyses of global ssVEP amplitude revealed main effects of CS Type [$F(1,14) = 7.14$, $P = 0.018$, $\eta_p^2 = 0.34$] and Trial Type [$F(1,14) = 8.98$, $P = 0.01$, $\eta_p^2 = 0.39$]. As illustrated in Figure 1C, total ssVEP amplitude scaled additively across the four experimental conditions—the greatest visuocortical engagement was observed for the CS+ trials when threat could be avoided and the smallest engagement was observed for CS− trials with no action-related requirements. The remaining conditions exhibited intermediate levels of ssVEP amplitude.

#### *CS+/CS− processing (CS cue frequency tag)*

Examination of the electrocortical responses evoked by the conditioned grating stimuli revealed a main effect of CS Type [$F(1,14) = 6.27$, $P = 0.025$, $\eta_p^2 = 0.31$], but no CS Type × Trial Type ($F < 1$) interaction. The results confirm the visual impression conveyed by Figure 2 that the CS+ cues evoked larger ssVEP amplitudes relative

to the CS− cues regardless of whether the harmful outcome was capable of being avoided or not.

To further test the hypothesis that CS+ cues evoked greater visuocortical activity than that of the CS− cues, we also conducted two planned contrasts. Directional, one-tailed paired-sample *t*-tests revealed increased amplitude for the CS+ cue relative to the CS−, both when the UCS delivery was avoidable [$t(14) = 2.08$, $P = 0.028$] and when it was unavoidable [$t(14) = 2.11$, $P = 0.027$]. Table 1 depicts the means and standard errors for each experimental condition.

### *Trial-Type processing (action cue frequency tag)*

As indicated in Figure 3, visuocortical response amplitude was strongly enhanced for peripheral cues that signaled an active response compared with the cues signaling a passive trial with no motor component. A main effect of Trial Type [$F(1,14) = 14.34$, $P = 0.002$, $\eta_p^2 = 0.51$] provides statistical support for this interpretation. The absence of effects involving CS Type ($F$s < 1) further suggests amplitude modulation driven by motor demands was orthogonal to affective influences related to the aversive conditioning.

When modeling the intracortical sources of the scalp recorded ssVEPs, our analysis revealed a signal origin within the visual cortex for both frequency tagged stimuli (Figures 2 and 3 insets), consistent with previous evidence that ssVEP responses propagate mostly from dipoles located deep within the calcarine fissure.

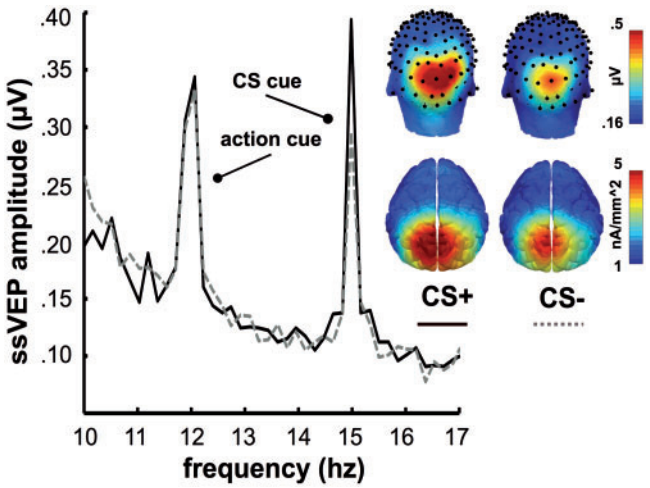


**Fig. 2** Grand mean power spectrum for the CS+ (black solid) and CS− (gray dashed) conditions from an averaged pool of posterior sensors surrounding Oz, collapsing across active and passive conditions. Also depicted is the topographical distribution (mapped with spherical splines) of the grand mean grating-evoked ssVEP amplitudes in sensor space (heads, back view). The schematic brains (back view) depict source strength amplitude, revealing an inverse MN solution with signal origin in visual cortex.

**Table 1** Mean (s.e.m.) posterior ssVEP amplitudes (in μV) for each condition of the avoidance phase averaged over the viewing period (1–6 s post-stimulus onset)

| | 15 Hz—grating tag | 12 Hz—peripheral cue tag |
|---|---|---|
| Active CS+ | 0.38 (0.09) | 0.44 (0.06) |
| Active CS− | 0.29 (0.06) | 0.40 (0.06) |
| Passive CS+ | 0.42 (0.09) | 0.25 (0.03) |
| Passive CS− | 0.31 (0.06) | 0.27 (0.03) |

### *Response trade-off in visual cortex*

We next tested whether the trade-off in terms of population-level responses was resolved in favor of the conditioned grating or the peripheral action cues.

When contrasting ssVEP amplitudes evoked by the conditioned cues, there was a CS Type × Tagged Stimulus interaction [$F(1,14) = 5.02$, $P = 0.042$, $\eta_p^2 = 0.26$]. For the active/passive comparison, there was similarly an interaction between Trial Type and Tagged Stimulus [$F(1,14) = 12.56$, $P = 0.003$, $\eta_p^2 = 0.47$]. We next computed a set of trade-off indices (ΔssVEP amplitude = action cue tag amplitude − grating tag amplitude) where negative scores indicate relatively greater grating-evoked response amplitudes and positive scores denote relatively greater action cue-evoked amplitudes. As illustrated in Figure 4, CS+ trials compared with CS− trials led to the response trade-off being resolved in favor of relatively greater grating-evoked amplitude [$t(14) = -2.24$, $P = 0.04$]. Response trade-off on the active, compared with passive, trials was resolved in favor of greater action cue-evoked amplitudes [$t(14) = 3.54$, $P = 0.003$].

### Long range phase synchronization

When examining long-range phase synchronization at the driving frequency of the conditioned gratings (15 Hz), the analysis revealed a number of source regions exhibiting increased long-range phase synchronization with the visual seed region during the active CS+ compared with the active CS− trials (Figure 5). In addition to a cluster of sources within the parieto-occipital cortex, bilateral sources roughly corresponding to the pre-motor and motor strips, as well as within the frontal cortex revealed increased functional connectivity with the visual cortex. No other comparisons survived the permutation-based significance thresholds.

When testing the spatial topography of phase synchronization at the frequency of the peripheral action cues (12 Hz), parieto-occipital regions falling within the dorsal visual pathway showed increased synchrony with the visual cortex during the processing of cues signaling action requirements compared with those indicating a passive trial (Figure 6). Additionally, sources in the frontal cortex also exhibited increased phase synchrony with the visual cortex during the active, compared with the passive, trials.

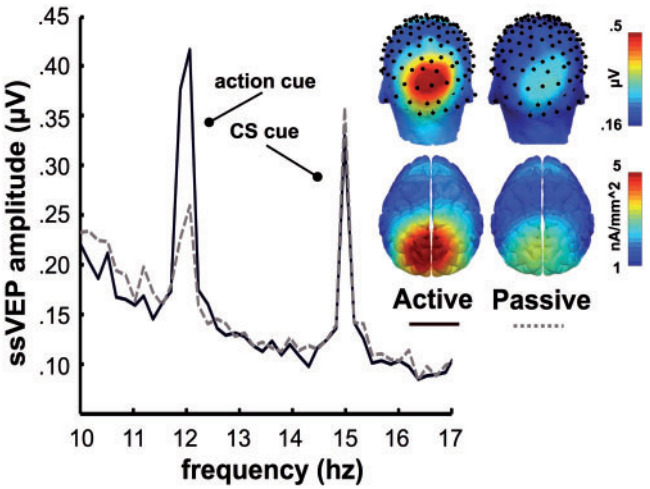


**Fig. 3** Grand mean power spectrum for the active (black solid) and passive (gray dashed) conditions from an averaged pool of posterior sensors surrounding Oz, collapsing across CS+ and CS− conditions. Topographic plots were constructed as in Figure 2.

## DISCUSSION

Threat-related cues elicited stronger population responses within visual cortex than did the safety cues. Population activity was also enhanced in response to cues that indicated an active behavioral response compared with those signaling passive viewing. In terms of overall responding driven by the global stimulus array, we observed the strongest engagement of visual cortical networks when viewing threat-related cues where the associated aversive outcomes could be avoided by a simple behavior. Considered together, the findings suggest that response gain in visual neuron populations was modulated in an additive rather than interactive fashion. The emotional significance of stimuli and top-down instructions served to enhance visual cortical responses in parallel.

Examining neuronal responses evoked by the conditioned gratings in isolation from the global stimulus array revealed that the threat-related grating elicited stronger ssVEP amplitudes than the safety cue, even when the negative outcome could be avoided by a motor response. This latter finding is in contrast to the observation that such trials were experienced as less distressing compared with those where aversive stimulus delivery was unavoidable. Previous experiments have reported that avoidance behaviors reduce autonomic indices of fearful arousal in similar laboratory models (e.g. Lovibond *et al.*, 2008).

Although it could be argued that the visual processing of threat-related stimuli extinguishes as the avoidance response itself becomes over-learned, it is important to note that participants in our study were explicitly instructed about the efficiency of instrumental avoidance and did not have to rely solely on previous experience to acquire an instrumental response. Thus, it seems unlikely that insufficient learning could have explained our ssVEP findings.

As previously mentioned, evidence from fMRI studies suggests that there is lingering amygdala activation for threat cues, even when negative outcomes are consistently avoided (Schlund and Cataldo, 2010; Schlund *et al.*, 2010), indicating persistent strengthening of neural activity in defensive circuits. Our results extend these findings to the human visual cortex, suggesting that response gain for threat-related stimuli is not easily extinguished by avoidance responses. Although these findings may seem surprising from the perspective that conditioned responding reflects a net sum of excitatory and inhibitory influences (Rescorla, 1969), it is consistent with contemporary perspectives that avoidance responses can serve to preserve threat beliefs (Lovibond *et al.*, 2009). Attributing reprieve from a negative outcome to self-initiated actions allows the conditioned cue's aversive association to remain intact. The findings here are also consistent with previous evidence that a visual response bias for threat-related cues survives an inhibitory transfer test (Miskovic and Keil, 2013).

The observation that ssVEP amplitude modulations for the threat-related gratings and action cues operated in an additive fashion is consistent with theoretical models postulating the existence of multiple and parallel sources of biases in sensory processing (Pourtois *et al.*,

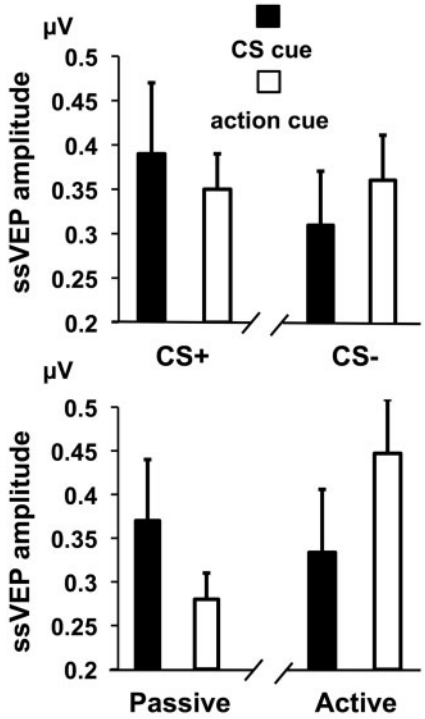


**Fig. 4** Grand mean bar plots of raw ssVEP amplitudes during the last half of stimulus presentation for each of the two tagged stimuli, illustrating the effects due to conditioning (top) and action context (bottom). Bars depict + 1 s.e.m.

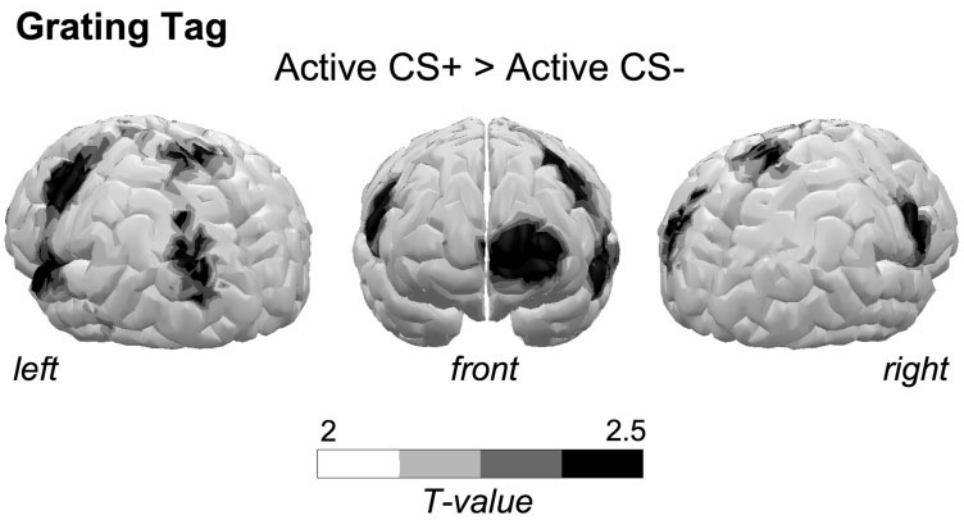


**Fig. 5** Distribution of *t*-test values plotted on a cortical surface rendering. Dark colors indicate regions that showed enhanced phase synchronization with the visual cortex at the driving frequency of 15 Hz, corresponding to the conditioned grating. The critical *t*-test values for a significance level of $P < 0.05$ were determined using a permutation-based procedure with a total of 8000 condition permutations.

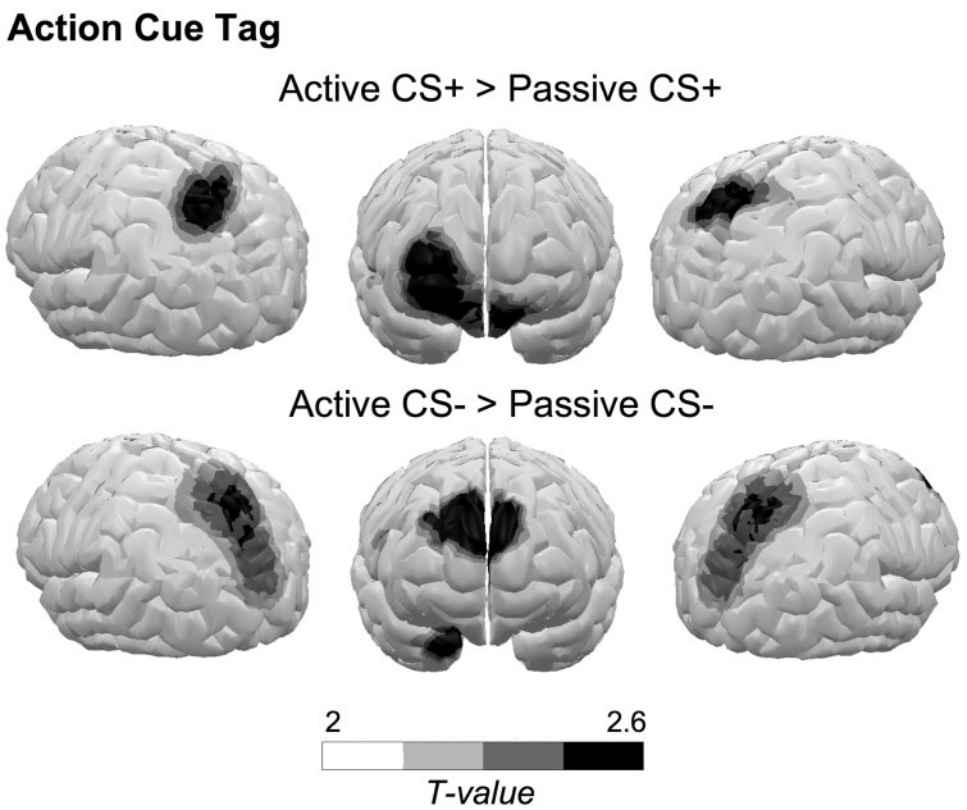


**Fig. 6** Distribution of *t*-test values on a cortical surface rendering. Dark colors indicate regions that showed enhanced phase synchronization with the visual cortex at the driving frequency of 12 Hz, corresponding to the action cues. The critical *t*-test values for a significance level of $P < 0.05$ were determined using a permutation-based procedure with a total of 8000 condition permutations.

2013). In short, sensory features encountered in the environment become relevant (and elicit more robust neuronal responses) for different reasons: the emotional significance of stimuli or cognitive strategies that are voluntarily adapted to optimize performance in given situations. Presumably, although the downstream effects are expressed in similar ways (i.e. response enhancement in sensory cortex), the underlying sources for such effects originate from distinct neural structures—deep brain nuclei responsible for imbuing sensoria with emotional significance *vs* cortical networks that implement flexible top-down templates. Interestingly, when examining brain activity evoked by the action cues, there was no evidence that the shapes signaling the capacity to terminate a negative outcome elicited greater activity than the shapes that were rendered behaviorally relevant by simple task instruction. In other words, there is no evidence that the visual system responds preferentially to features that one might predict would qualify as safety stimuli (see also Miskovic and Keil, 2013).

We observed two main findings in terms of competition between neuronal populations entrained to the driving frequencies of the conditioned gratings *vs* action cues. First, taken overall, the CS+ led to stronger responses of visual neurons relative to the action cues; in contrast, the CS− cue produced weaker population responses relative to the peripheral stimuli. Second, the peripheral cues evoked greater responses overall relative to the central gratings, when the peripheral cues served as proximal signals for a motor response; in contrast, when the peripheral cues were devalued by removing the need for a signaled overt response, electrocortical response strength shifted in favor of the centrally presented grating stimuli.

Beyond local population activity in the visual cortex, our results revealed specific patterns of stimulus driven large-scale network configuration during motivated avoidance. The strength of phase synchrony between the visual cortex and regions of the parietal, pre-motor/motor and frontal cortices increased when individuals viewed threat-related, compared with safety gratings in an action context. Many of the regions showing threat-specific enhancement during the active avoidance condition overlapped with regions that have previously demonstrated heightened coupling with the visual cortex during the viewing of affectively arousing images (Keil *et al.*, 2009, 2012). The additional cortical structures that interacted with the visual source regions of interest are those likely to be involved in linking perceptual features of the threat-related stimulus with attentive behavior and action preparation. It is instructive to highlight the point that differences in visual–extravisual coupling during the viewing of threat and safety gratings emerged only in the context of active perception, where there was involvement of motor responses. The observation that the strength of this stimulus driven oscillatory communication was higher when the outcome of the behavioral performance produced a motivationally relevant outcome in the environment (by terminating the delivery of an unpleasant event) provides support for the suggestion that aversive conditioning is intimately connected with action dispositions of avoidance and withdrawal (Beckers *et al.*, 2013). In terms of the neural activity evoked by the peripheral cues, regions falling within the dorsal pathway and the frontal cortex showed stronger synchronization with the visual cortex during the active motor compared with the passive viewing condition, adding further support for enhanced functional integration between widely distributed neuronal ensembles during perception–action coupling.

Taken together, our findings provide evidence for a cascade of neuroelectric events, originating within the visual cortex and extending beyond it, that accompany behavioral confrontation with threat-related sensory features. By situating aversive conditioning in a more naturalistic experimental setting—where participants take active steps

to minimize the likelihood of unpleasant outcomes rather than being passive observers—our study links motivated visual brain function to its behavioral consequences. Although this study focused on aversive conditioning, it is possible that similar principles might be observed in future studies that focus on reward or appetitive signal processing.

## REFERENCES


Andersen, S.K., Müller, M.M. (2010). Behavioral performance follows the time course of neural facilitation and suppression during cued shifts of feature-selective attention. *Proceedings of the National Academy of Sciences of the United States of America*, *107*, 13878–82.

Barrett, L.F., Bar, M. (2009). See it with feeling: affective predictions during object perception. *Philosophical Transactions of the Royal Society of London, Series B, Biological Sciences*, *364*, 1325–44.

Beckers, T., Krypotos, A.M., Boddez, Y., Effting, M., Kindt, M. (2013). What's wrong with fear conditioning? *Biological Psychology*, *92*, 90–6.

Blair, R.C., Karniski, W. (1993). An alternative method for significance testing of waveform difference potentials. *Psychophysiology*, *30*, 518–24.

Brainard, D.H. (1997). The psychophysics toolbox. *Spatial Vision*, *10*, 433–6.

Delgado, M.R., Jou, R.L., LeDoux, J.E., Phelps, E.A. (2009). Avoiding negative outcomes: tracking the mechanisms of avoidance learning in humans during fear conditioning. *Frontiers in Behavioral Neuroscience*, *3*, 33.

Engel, A.K., Fries, P., Singer, W. (2001). Dynamic predictions: oscillations and synchrony in top-down processing. *Nature Reviews Neuroscience*, *2*, 704–16.

Engel, A.K., Maye, A., Kurthen, M., König, P. (2013). Where's the action? The pragmatic turn in cognitive science. *Trends in Cognitive Science*, *17*, 202–9.

Freeman, W. (2001). *How Brains Make Up Their Minds*. New York, NY: Columbia University Press.

Gallant, J.L., Connor, C.E., Van Essen, D.C. (1998). Neural activity in areas V1, V2 and V4 during free viewing of natural scenes compared to controlled viewing. *NeuroReport*, *9*, 2153–8.

Gilbert, C.D., Sigman, M. (2007). Brain states: top-down influences in sensory processing. *Neuron*, *54*, 677–96.

Hauk, O. (2004). Keep it simple: a case for using classical minimum norm estimation in the analysis of EEG and MEG data. *NeuroImage*, *21*, 1612–21.

Hauk, O., Keil, A., Elbert, T., Müller, M. (2002). Comparison of data transformation procedures to enhance topographical accuracy in time-series analysis of the human EEG. *Journal of Neuroscience Methods*, *113*, 111–22.

Junghöfer, M., Elbert, T., Tucker, D.M., Rockstroh, B. (2000). Statistical control of artifacts in dense array EEG/MEG studies. *Psychophysiology*, *37*, 523–32.

Keil, A., Costa, V., Smith, J.C., et al. (2012). Tagging cortical networks in emotion: a topographical analysis. *Human Brain Mapping*, *33*, 2920–31.

Keil, A., Sabatinelli, D., Ding, M., Lang, P.J., Ihssen, N., Heim, S. (2009). Re-entrant projections modulate visual cortex in affective perception: directional evidence from Granger causality analysis. *Human Brain Mapping*, *30*, 532–40.

Keil, A., Smith, J.C., Wangelin, B.C., Sabatinelli, D., Bradley, M.M., Lang, P.J. (2008). Electrocortical and electrodermal responses covary as a function of emotional arousal: a single-trial analysis. *Psychophysiology*, *45*, 516–23.

Kim, H., Shimojo, S., O'Doherty, J.P. (2006). Is avoiding an aversive outcome rewarding? The neural substrates of avoidance learning in the human brain. *PLoS Biology*, *4*, e233.

Lachaux, J.P., Rodriguez, E., Martinerie, J., Varela, F.J. (1999). Measuring phase synchrony in brain signals. *Human Brain Mapping*, *8*, 194–208.

Lang, P.J., Bradley, M.M. (2010). Emotion and the motivational brain. *Biological Psychology*, *84*, 437–50.

LeDoux, J.E., Gorman, J.M. (2001). A call to action: overcoming anxiety through active coping. *American Journal of Psychiatry*, *158*, 1953–5.

Lee, T.S., Yang, C.F., Romero, R.D., Mumford, D. (2002). Neural activity in early visual cortex reflects behavioral experience and higher-order perceptual salience. *Nature Neuroscience*, *5*, 589–97.

Lohr, J.M., Olatunji, B.O., Sawchuk, C.N. (2007). A functional analysis of danger and safety signals in anxiety disorders. *Clinical Psychology Review*, *27*, 114–26.

Lovibond, P.F., Mitchell, C.J., Minard, E., Brady, A., Menzies, R.G. (2009). Safety behaviours preserve threat beliefs: protection from extinction of human fear conditioning by an avoidance response. *Behaviour Research and Therapy*, *47*, 716–20.

Lovibond, P.F., Saunders, J.C., Weidemann, G., Mitchell, C.J. (2008). Evidence for expectancy as a mediator of avoidance and anxiety in a laboratory model of human avoidance learning. *The Quarterly Journal of Experimental Psychology*, *61*, 1199–216.

Mirabella, G., Bertini, G., Samengo, I., et al. (2007). Neurons in area V4 of the macaque translate attended visual features into behaviorally relevant categories. *Neuron*, *54*, 303–18.

Miskovic, V., Keil, A. (2013). Perceiving threat in the face of safety: excitation and inhibition of conditioned fear in human visual cortex. *The Journal of Neuroscience*, *33*, 72–8.

Moratti, S., Keil, A. (2005). Cortical activation during Pavlovian fear conditioning depends on heart rate response patterns: an MEG study. *Cognitive Brain Research*, *25*, 459–71.

Moratti, S., Keil, A., Miller, G.A. (2006). Fear but not awareness predicts enhanced sensory processing in fear conditioning. *Psychophysiology*, *43*, 216–26.

Müller, M.M., Andersen, S.K., Keil, A. (2008). Time course of competition for visual processing resources between emotional pictures and foreground task. *Cerebral Cortex*, *18*, 1892–9.

Müller, M.M., Teder-Sälejärvi, W., Hillyard, S.A. (1998). The time course of cortical facilitation during cued shifts of spatial attention. *Nature Neuroscience*, *1*, 631–4.

Niell, C.M., Stryker, M.P. (2010). Modulation of visual responses by behavioral state in mouse visual cortex. *Neuron*, *65*, 472–9.

Nunez, P.L., Srinivasan, R. (2006). *Electric Fields of the Brain: The Neurophysics of EEG, 2nd edn*. New York, NY: Oxford University Press.

Peyk, P., De Cesarei, A., Junghöfer, M. (2011). ElectroMagnetoEncephalography software: overview and integration with other EEG/MEG toolboxes. *Computational Intelligence and Neuroscience*, *2011*, 861705.

Pourtois, G., Schettino, A., Vuilleumier, P. (2013). Brain mechanisms for emotional influences on perception and attention: what is magic and what is not. *Biological Psychology*, *92*, 492–512.

Rachman, S. (1977). The conditioning theory of fear acquisition: a critical examination. *Behavioural Research Therapy*, *15*, 375–87.

Regan, D. (1989). *Human Brain Electrophysiology: Evoked Potentials and Evoked Magnetic Fields in Science and Medicine*. New York, NY: Elsevier.

Rescorla, R.A. (1969). Pavlovian conditioned inhibition. *Psychological Bulletin*, *72*, 77–94.

Schlund, M.W., Cataldo, M.F. (2010). Amygdala involvement in human avoidance, escape and approach behaviour. *Neuroimage*, *53*, 769–76.

Schlund, M.W., Hudgins, C.B., Magee, S., Dymond, S. (2013). Neuroimaging the temporal dynamics of human avoidance to sustained threat. *Behavioural Brain Research*, *257*, 148–55.

Schlund, M.W., Siegle, G.J., Ladouceur, C.D., et al. (2010). Nothing to fear? Neural systems supporting avoidance behavior in healthy youths. *Neuroimage*, *52*, 710–9.

Schoffelen, J.-M., Gross, J. (2009). Source connectivity analysis with MEG and EEG. *Human Brain Mapping*, *30*, 1857–65.

Szpiler, J.A., Epstein, S. (1976). Availability of an avoidance response as related to autonomic arousal. *Journal of Abnormal Psychology*, *85*, 73–82.

Tononi, G., Srinivasan, R., Russell, D.P., Edelman, G.M. (1998). Investigating neuronal correlates of conscious perception by frequency-tagged neuromagnetic responses. *Proceedings of the National Academy of Sciences of the United States of America*, *17*, 3198–203.

Vialatte, F.-B., Maurice, M., Dauwels, J., Cichocki, A. (2010). Steady-state visually evoked potentials: focus on essential paradigms and future perspectives. *Progress in Neurobiology*, *90*, 418–38.

Weinberger, N.M. (2004). Specific long-term memory traces in primary sensory cortex. *Nature Reviews Neuroscience*, *5*, 279–90.

Wieser, M.J., Keil, A. (2011). Temporal trade-off effects in sustained attention: dynamics in visual cortex predict the target detection performance during distraction. *The Journal of Neuroscience*, *31*, 7784–90.

van Swinderen, B., Greenspan, R.J. (2003). Salience modulates 20-30 Hz brain activity in *Drosophila*. *Nature Neuroscience*, *6*, 579–86.